Solvent and Pressure Effects on Quenching by Oxygen of 9,10-Dimethylanthracene Fluorescence in Liquid *n*-Alkanes: A Study on Solvent Cage Effects

Masami Okamoto*,† and Fujio Tanaka‡

Faculty of Engineering and Design, Kyoto Institute of Technology, Matsugasaki, Sakyo-ku, Kyoto 606-8585, Japan, and Department of Chemistry, Graduate School of Science, Osaka Prefecture University, Gakuen-cho, Sakai 599-8531, Japan

Received: April 24, 2006; In Final Form: July 23, 2006

The fluorescence quenching by oxygen of 9,10-dimethylanthracene (DMEA) in liquid ethane and propane at pressures up to 60 MPa and 25 °C was investigated. The apparent activation volumes for the quenching rate constant, k_q, $\Delta V_q^{\ddagger}$, were 5.0 ± 3.4 and 7.4 ± 1.0 cm^3/mol, whereas those for the solvent viscosity, η, $\Delta V_\eta^{\ddagger}$, were 190 ± 22 and 42 ± 1 cm^3/mol in ethane and propane at 6.0 MPa, respectively. These results were discussed together with those in *n*-alkanes (C_4−C_7) and methylcyclohexane (MCH) that were previously reported, and it was found that $\Delta V_q^{\ddagger}$ increases monotonically but $\Delta V_\eta^{\ddagger}$ decreases rapidly with increasing the number of carbon atoms in *n*-alkanes. The plot of ln k_q against ln η showed a leveling-off with decreasing η. These observations were analyzed satisfactorily by the pressure dependence of the solvent viscosity on k_q coupled with that of the radial distribution function, $g(\sigma)$, at contact with a hard sphere assumption. The apparent bimolecular rate constant, $k_{bim,0}$, for the quenching in the solvent cage was evaluated by extrapolating to $g(\sigma)\eta = 0$ in the plot of $g(\sigma)/k_q$ against $g(\sigma)\eta$, and it was found that $k_{bim,0}$ decreased with increasing the radius of the solvent molecule. From the solvent size dependence of $k_{bim,0}$, the solvent cage effect was discussed phenomenologically.

Introduction

Because of the photochemical and photobiological importance, the quenching by oxygen of the lowest electronically excited molecules of the singlet (S_1) and triplet (T_1) states, which is followed by the formation of singlet oxygen, has been extensively investigated.[1−6] It is well-known that the fluorescence of many aromatic hydrocarbons is quenched by oxygen with a nearly diffusion rate constant, k_{diff}, since the rate constant for the quenching, k_q, is approximately equal to k_{diff} calculated in a continuum medium with viscosity, η, by the Debye equation[1−5]

$$k_{diff} = 8RT/\alpha\eta \tag{1}$$

where α is 2000 and 3000 for the slip and stick boundary limits, respectively.

High pressure is a powerful tool to investigate the nearly diffusion-controlled and/or diffusion-controlled reaction since it can change the solvent viscosity significantly and continuously without changing solvent and temperature. Recently, we systematically investigated the quenching of the S_1 state of some aromatic molecules by the quenchers including oxygen as a function of pressure and found that k_q is not described by eq 1 at high pressure as well as at 0.1 MPa.[7−14] For oxygen quenching of the fluorophore, ^{1}M*, we adopted a conventional scheme (Scheme 1) as the quenching mechanism where $(^1M^*O_2)_{en}$ is an encounter complex between ^{1}M* and O_2 in the solvent cage, and k^S is the unimolecular rate constant of deactivation of $(^1M^*O_2)_{en}$ in the solvent cage.

SCHEME 1

$$^1M^* + O_2 \underset{k_{-diff}}{\overset{k_{diff}}{\rightleftarrows}} (^1M^*O_2)_{en} \xrightarrow{k^S} \text{quenching}$$

According to Scheme 1, the observed quenching rate constant, k_q, may be given by eq 2.

$$k_q = \frac{k_{diff}k^S}{k_{-diff} + k^S} \tag{2}$$

We assume that the rate constant for diffusion, k_{diff}, is expressed by a modified Debye equation, eq 3, which is similar to eq 1.

$$k_{diff} = 8RT/\alpha^{ex}\eta \tag{3}$$

In eq 3, α^{ex} is a constant determined experimentally.[16,17,20−22,24] From eqs 2 and 3, we have eq 4.

$$\frac{1}{k_q} = \frac{1}{k^S}\left(\frac{k_{-diff}}{k_{diff}}\right) + \frac{\alpha^{ex}}{8RT}\eta \tag{4}$$

In eq 4, the pressure dependence of k_{diff}/k_{-diff} may be given by that of the radial distribution function, $g(\sigma)$, at the closest approach distance, σ (= $r_{M^*} + r_O$; the sum of the radius of ^{1}M*, r_{M^*}, and oxygen molecule, r_O, with hard spheres)

$$\frac{\gamma}{k_q} = \frac{1}{k_{bim}^0} + \frac{\alpha^{ex}}{8RT}(\gamma\eta) \tag{5}$$

where γ is the ratio of $g(\sigma)$ (= $g(\sigma)_P/g(\sigma)_{Pref}$) at P MPa to that at a given reference pressure, P_{ref}, normally, P_{ref} = 0.1 MPa.

* To whom correspondence should be addressed.
† Kyoto Institute of Technology.
‡ Osaka Prefecture University.

10.1021/jp062517o CCC: $33.50
Published on Web 08/23/2006

In eq 5 k^0_{bim} is determined by extrapolating to $\gamma\eta = 0$ in the plot of γ/k_q against $\gamma\eta = 0$, i.e., $k^0_{bim} = k^S(k_{diff}/k_{-diff})_{\gamma\eta \to 0}$. Thus, k^0_{bim} is given by the product of k^S and $(k_{diff}/k_{-diff})_{\gamma\eta \to 0}$ that has the unit of M^{-1} s^{-1}, and hence, we define k^0_{bim} as the apparent bimolecular quenching rate constant in the solvent cage at a reference state, $g(\sigma)_{Pref}$, since k^0_{bim} has the same unit as the bimolecular rate constant.

According to eq 5, the plot of γ/k_q against $\gamma\eta$ should be linear when k^0_{bim} and α^{ex} are independent of pressure. In fact, eq 5 was successfully applied for various quenching systems in supercritical fluids[17,19] as well as in liquids,[15−17,19−22] except for the fluorescence quenching of 9-cyanoanthracene by oxygen in supercritical carbon dioxide.[23] Thus, the pressure dependence of k_q revealed that the quenching of the S_1 state is not fully but nearly diffusion-controlled for various quenching systems.[15−25]

In this work, we investigated the fluorescence quenching by oxygen of 9,10-dimethylanthracene (DMEA) in various solvents including liquefied gases such as ethane, propane, and *n*-butane in order to characterize experimentally the oxygen quenching in the solvent cage since the bimolecular quenching in the solvent cage is supposed to depend significantly on the solvent properties such as size, density, and viscosity. For this purpose, we should introduce $g(\sigma)_{Pref}$ common to the solvents examined since k^0_{bim} in eq 5 depends on $g(\sigma)_{Pref}$. In this work, as a new reference state, we selected $g(\sigma)_{Pref} = 1$ that corresponds to the radial distribution function at contact in gas phase. Thus, we modified eq 5 as follows:

$$\frac{g(\sigma)}{k_q} = \frac{1}{k_{bim,0}} + \frac{\alpha^{ex}}{8RT}(g(\sigma)\eta) \qquad (6)$$

where $k_{bim,0}$ is redefined as the value at $g(\sigma)\eta \to 0$, $k_{bim,0} = k^S(k_{diff}/k_{-diff})_{g(\sigma)\eta \to 0}$. As for k^0_{bim} mentioned above, $k_{bim,0}$ is given by the product of k^S and $(k_{diff}/k_{-diff})_{g(\sigma)\eta \to 0}$ and defined as the apparent bimolecular quenching rate constant in the solvent cage at a reference state, $g(\sigma) = 1$. Consequently, the difference between k^0_{bim} in eq 5 and $k_{bim,0}$ in eq 6 is attributed to that in the reference state, which is the value, $g(\sigma)_{Pref}$, at a given pressure, P_{ref}, for the former and $g(\sigma) = 1$ for the latter. It is noticed that α^{ex} determined by eq 6 is the same value as that by eq 5, and $k_{bim,0}$ (eq 6) is equal to $k^0_{bim}/g(\sigma)_{Pref}$. In this work, we measured k_q for DMEA/O_2 in liquid ethane and propane for which the size, the viscosity, and the density at a given pressure are smaller than those for the solvents studied previously.[17,20,21] The results, together with those in other *n*-alkanes and methylcyclohexane (MCH) reported previously, are analyzed by eq 6, and the solvent and pressure (density) dependence of the apparent bimolecular quenching rate constant, $k_{bim,0}$, in solvent cage as well as the competition of the quenching with diffusion is discussed.

Experimental Section

9,10-Dimethylanthracene (DMEA) (Aldrich Chemical Co.) was recrystallized from methanol and then purified by thin-layer chromatography. Ethane and propane (Sumitomo Seika; purity, 99.995%) were used as received.

Fluorescence decay curve measurements at high pressure were performed by using a 0.3-ns pulse from a PRA LN103 nitrogen laser for excitation. The fluorescence intensities were measured by a Hamamatsu R1635-02 photomultiplier through a Ritsu MC-25NP monochromator, and the resulting signal was digitized by using a LeCroy 9362 digitizing oscilloscope. All data were analyzed by using a NEC 9801 microcomputer, which was interfaced to the digitizer. The associated high-pressure techniques have been described in detail elsewhere.[17,19,23,26]

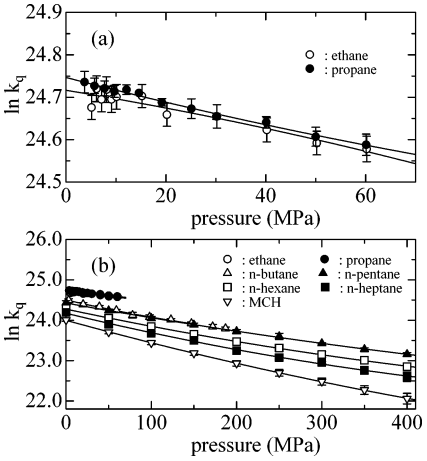

Figure 1. Pressure dependence of k_q in ethane and propane (a) and *n*-alkanes (C_2−C_7) and methylcyclohexane (MCH) (b) at 25 °C. In panel b, the plot for ethane is overlapping with that for propane.

The sample solution of DMEA in ethane and propane with oxygen was prepared as follows. An appropriate volume of a hexane stock solution of DMEA was placed into a high-pressure cell with four optical sapphire windows. The solvent was evaporated, and the high-pressure cell was evacuated and then filled with ethane or propane from a high-pressure syringe pump (500 MPa). The oxygen concentration was determined by introducing a known pressure of synthesized air (oxygen/ nitrogen/ argon = 21/78/1 vol %, Taiyo Oxygen Co.) into the high-pressure cell. The absorbance of DMEA for the fluorescence lifetime measurements was less 0.1 (1 cm-cell) at the maximum absorption wavelength in order to minimize the reabsorption effects. Complete dissolution of oxygen in liquid was checked by measuring the fluorescence lifetime of DMEA as a function of time.

Temperature was controlled at 25 ± 0.1 °C. Pressure was measured by a Nagano Keiki Seisakusho KH15 (68.6 MPa) strain gauge.

Results

Fluorescence quenching was examined in the absence and presence of O_2 in ethane and propane at 25 °C. The decay curves were satisfactorily analyzed by a single-exponential function in all of the conditions examined. The lifetimes in the absence of the quencher, τ^0_f, were found to be 16.0 and 16.2 ns in liquid ethane and propane at 25 °C and 6.0 MPa, respectively. They are close to those in *n*-alkanes (C_4−C_7) and methylcyclohexane at 25 °C and 0.1 MPa (13.8−15.0 ns).[17] The values of τ^0_f were found to decrease slightly with increasing pressure; they were 14.6 ns and 15.3 ns at a pressure of 60 MPa in ethane and propane at 25 °C, respectively. The value of k_q was determined by the plot of $1/\tau_f$ as a function of the concentration of O_2, [O_2] (five concentrations), according to eq 7.

$$1/\tau_f - 1/\tau^0_f = k_q[O_2] \qquad (7)$$

Figure 1 shows the pressure dependence of k_q in ethane and propane (Figure 1a), together with that in *n*-alkanes (C_2−C_7) and MCH (Figure 1b) at 25 °C reported previously. It can be seen that k_q decreases more significantly with increasing the number of carbons in *n*-alkanes. The apparent activation volumes for k_q, $\Delta V^{\ddagger}_q$, at 6.0 MPa evaluated by eq 8 are listed in Table 1, together with those for solvent viscosity, $\Delta V^{\ddagger}_{\eta}$,

TABLE 1: Values of Activation Volume (cm³/mol), $\Delta V_q^{\ddagger}$ and $\Delta V_\eta^{\ddagger}$, and β (mean) Associated with Fluorescence Quenching of DMEA by Oxygen in *n*-Alkanes and MCH at 25 °C

solvent	$\Delta V_q^{\ddagger}$ [a]	$\Delta V_\eta^{\ddagger}$ [a,b]	β (mean)[c]
ethane	5.0 ± 3.4	190 ± 22	0.14 ± 0.03
propane	7.4 ± 1.0	42 ± 1	0.26 ± 0.02
n-butane	11.9 ± 1.0	24 ± 1	0.59 ± 0.02
n-pentane	9.4 ± 0.3	18 ± 1	0.64 ± 0.03
n-hexane	11.0 ± 0.2	18 ± 2	0.70 ± 0.03
n-heptane	12.6 ± 0.7	21 ± 1	0.64 ± 0.02
MCH	14.3 ± 0.2	23 ± 1	0.66 ± 0.01

[a] Values at 6.0 MPa. [b] Values of $\Delta V_\eta^{\ddagger}$ were determined according to the equation $(\partial \ln \eta/\partial P)_T = \Delta V_\eta^{\ddagger}/RT$. [c] Mean values were determined from the slopes of the linear plot of ln k_q against ln η.

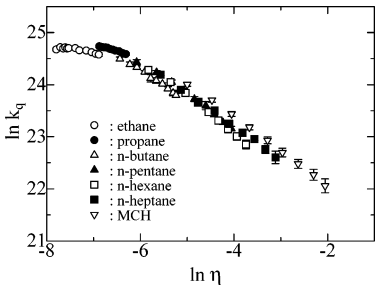

Figure 2. Solvent viscosity dependence of k_q in *n*-alkanes (C_2-C_7) and methylcyclohexane (MCH) at 25 °C.

calculated using the viscosity data.[27−37]

$$(\partial \ln k_q/\partial P)_T = -\Delta V_q^{\ddagger}/RT \quad (8)$$

It is found in Table 1 that the values of $\Delta V_q^{\ddagger}$ and $\Delta V_\eta^{\ddagger}$ are approximately constant in *n*-alkanes (C_4-C_7) and MCH although their individual magnitudes show significant differences. However, by comparison, $\Delta V_q^{\ddagger}$ values in ethane and propane are clearly smaller than $\Delta V_\eta^{\ddagger}$ values. It is also noted in Table 1 that $\Delta V_q^{\ddagger}$ increases but $\Delta V_\eta^{\ddagger}$ significantly decreases when the solvent is changed from ethane to propane. These results may be due to the difference in the degree of the contribution of the diffusion processes to the quenching.

In general, a fractional power dependence of k_q on η for the nearly diffusion-controlled reaction, which is given by eq 9, has often been observed

$$k_q = A\eta^{-\beta} \quad (9)$$

where A is a constant that is dependent on temperature, but independent of pressure, and β is less than unity. Figure 2 shows the solvent viscosity dependence of k_q in ethane and propane, together with the results in *n*-alkanes (C_4-C_7) and MCH reported previously.[17] It is found in Figure 2 that the plot of ln k_q against ln η is approximately linear in the solvents (C_4-C_7) and MCH with higher viscosity but clearly levels off in ethane and propane with lower viscosity as the solvent viscosity decreases. The mean values of β are listed in Table 1. As seen in Table 1, the values of β increase with increasing the number of carbon atoms in *n*-alkanes. These results indicate that the contribution of the diffusion processes to the quenching decreases with decreasing the solvent viscosity and the quenching seems to reach a rate characteristic of the quenching system (no contribution of diffusion) in the lower viscosity region; $k_q = (5.2 \pm 0.2) \times 10^{10}$ M^{-1} s^{-1} at the lowest η ($\eta = 0.041$ cP in ethane at 5.10 MPa and 25 °C) examined in this work. Thus, the observation implies that k_q has a limiting value independent of the solvent viscosity, that is, no contribution of diffusion to the quenching.

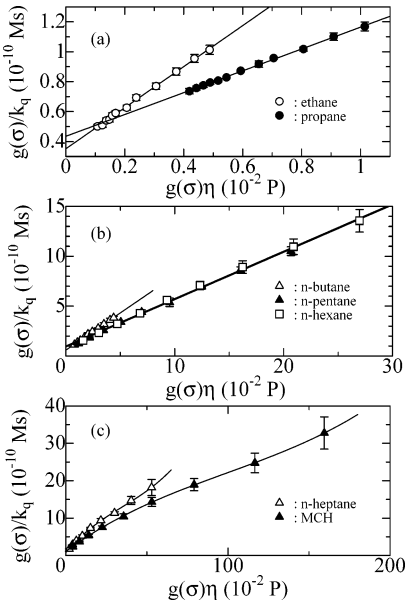

Figure 3. Plots of $k_q/g(\sigma)$ against $g(\sigma)\eta$ in ethane and propane (a), *n*-butane, *n*-pentane and *n*-hexane (b), and *n*-heptane and methylcyclohexane (MCH) (c) at 25 °C.

Discussion

We have previously studied the fluorescence quenching of DMEA by oxygen (DMEA/O_2) at high pressure in mainly normal solvents and showed phenomenologically and also from the analysis by eq 5 that the quenching is not fully but nearly diffusion-controlled.[16,17,19−22,24] In this work, all of the data including the results in *n*-alkanes (C_4-C_7) and methylcyclohexane (MCH) studied previously are analyzed by eq 6.

The plots of $g(\sigma)/k_q$ against $g(\sigma)\eta$ in *n*-alkanes and MCH are shown in Figure 3. As seen in panels a and b of Figure 3, the plots in ethane, propane, and *n*-alkanes (C_4-C_6) are approximately linear. The values of of α^{ex} and $k_{bim,0}$ were determined from the least squares slopes and intercepts for the plots in Figure 3, panels a and b, respectively, and listed in Table 2. However, the plots of $g(\sigma)/k_q$ against $g(\sigma)\eta$ in *n*-hepane and MCH with larger pressure dependence of η are not linear (Figure 3c). Such cases result from a translational-rotational coupling of diffusion in viscous solvents. We discussed this previously,[20] and α^{ex} was determined by assuming a polynominal in terms of $g(\sigma)\eta$ as follows:

$$\alpha^{ex} = \alpha_0 + \alpha_1(g(\sigma)\eta) + \alpha_2(g(\sigma)\eta)^2 + ... \quad (10)$$

Substituting eq 10 into eq 6, we have

$$\frac{g(\sigma)}{k_q} = \frac{1}{k_{bim,0}} + \frac{1}{8RT}[\alpha_0(g(\sigma)\eta) + \alpha_1(g(\sigma)\eta)^2 + \alpha_2(g(\sigma)\eta)^3 + ...] \quad (11)$$

The solid lines in Figure 3c were drawn by the approximation of a polynominal with the third order in terms of $g(\sigma)\eta$. The values of α^{ex} and $k_{bim,0}$ evaluated are also listed in Table 2.

Pressure and Solvent Dependence of α^{ex} and k_{diff}. The values of k_{diff} for *n*-alkanes (C_2-C_6) were determined by using α^{ex} (Table 2) and η, and those for *n*-heptane and MCH, for which the plots of $g(\sigma)/k_q$ against $g(\sigma)\eta$ are not linear, were evaluated by using α^{ex} obtained from the curve-fitting (see

TABLE 2: Fluorescence Quenching of DMEA by Oxygen in *n*-Alkanes and MCH at 25 °C[a]

solvent	r_s [a] (nm)	α^{ex}	$k_{bim,0}$ (10^{10} M^{-1} s^{-1})	$(k_{diff}/k_{-diff})_0$ [e] (M^{-1})	k^S (10^{11} s^{-1})
ethane	0.222	2720 ± 40[b]	2.85 ± 0.05[b]	0.195	1.46
propane	0.246	1450 ± 20[b]	2.30 ± 0.03[b]	0.158 ± 0.002	1.46 ± 0.04
n-butane	0.267	1480 ± 30[b]	1.71 ± 0.09[b]	0.117 ± 0.006	1.46 ± 0.15
n-pentane	0.285	940 ± 20[b]	1.10 ± 0.12[b]	0.075 ± 0.008	1.46 ± 0.30
n-hexane	0.301	940 ± 20[b]	1.00 ± 0.12[b]	0.069 ± 0.009	1.46 ± 0.35
n-heptane	0.315	990 ± 20[c,d]	1.26 ± 0.37[c]	0.086 ± 0.026	1.46 ± 0.86
MCH	0.304	620 ± 10[c,d]	0.90 ± 0.08[c]	0.062 ± 0.006	1.46 ± 0.24

[a] Values of r_{M^*} (0.365 nm), r_O (0.173 nm), and r_s were calculated by the method of Bondi.[40] [b] Values were determined by eq 6. [c] Values were determined by eq 11. [d] Values at 0.1 MPa. [e] Values were determined by assuming that $(\langle r^2 \rangle_0)^{1/2} = \sigma$ in ethane (see text).

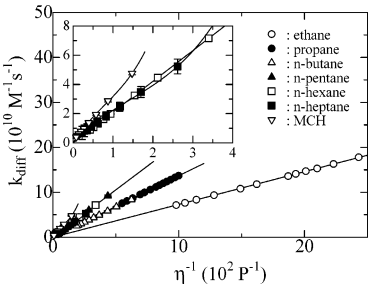

Figure 4. Plots of k_{diff} against η^{-1} in ethane ($k_{diff} = 0.730\eta^{-1}$), propane ($k_{diff} = 1.368\eta^{-1}$), *n*-butane ($k_{diff} = 1.341\eta^{-1}$), *n*-pentane ($k_{diff} = 2.109\eta^{-1}$), *n*-hexane ($k_{diff} = 2.105\eta^{-1}$), *n*-heptane ($k_{diff} = 0.194\eta^{-3} - 0.842\eta^{-2} + 2.876\eta^{-1}$), and methylcyclohexane ($k_{diff} = 0.817\eta^{-3} - 1.947\eta^{-2} + 4.304\eta^{-1}$) at 25 °C.

Figure 3c and eq 10) and η according to eq 3. The plots of k_{diff} thus determined against $1/\eta$ are shown in Figure 4.

In general, when the fluorophore, $^1M^*$, is quenched by O_2 with a diffusion rate in liquid solution, the bimolecular rate constant for diffusion, k_{diff}, is expressed by the relative diffusion coefficient D_{M^*O} ($= D_{M^*} + D_O$, sum of the diffusion coefficients for $^1M^*$ and O_2), and the closest approach distance, σ ($= r_{M^*} + r_O$) as follows:

$$k_{diff} = 4\pi\sigma N_A D_{M^*O}/10^3 \tag{12}$$

where N_A is Avogadro's number. The diffusion coefficient, D_i, for a solute molecule, *i*, of the spherical radius, r_i (i = M* or O), in a continuum medium with viscosity, η, is given by the Stokes−Einstein (SE) equation

$$D_i^{SE} = k_B T/f_i \pi r_i \eta \tag{13}$$

where $f_i = 4$ and 6 for the slip and stick boundary limits, respectively. Substituting eq 13 into eq 12, we have

$$k_{diff} = \frac{4\sigma RT}{10^3 \eta}\left(\frac{1}{f_{M^*} r_{M^*}} + \frac{1}{f_O r_O}\right) \tag{14}$$

By comparing eq 14 with eq 1, α is given by

$$\alpha = \frac{2 \times 10^3}{\sigma}\left(\frac{1}{f_{M^*} r_{M^*}} + \frac{1}{f_O r_O}\right)^{-1} \tag{15}$$

According to eq 15, α should be independent of the solvent, and 1750 for $f_{M^*} = f_O$ (=4), and 2620 for $f_{M^*} = f_O$ (=6). As seen in Table 2, the values of α^{ex} determined experimentally is close to stick boundary limit ($\alpha^{ex} = 2720$) in ethane, but seems to decrease with increasing the number of carbon atoms for *n*-alkanes. The large solvent dependence of α^{ex} may be due to the interactions between the solute and solvent molecules as well as their molecular sizes and shapes, which may change f_i (i = M* or O) for the real system. In fact, the measurements of

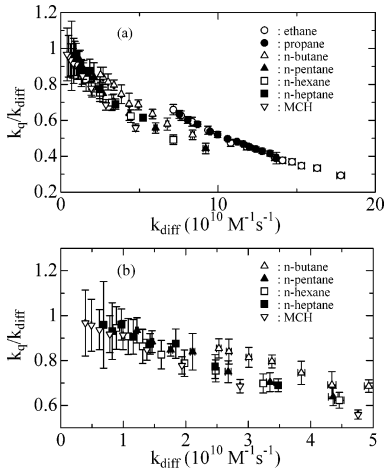

Figure 5. Plots of k_q/k_{diff} against k_{diff} in *n*-alkanes (C_2-C_7) and methylcyclohexane (MCH) (a) and *n*-alkanes (C_4-C_7) and MCH (b) at 25 °C.

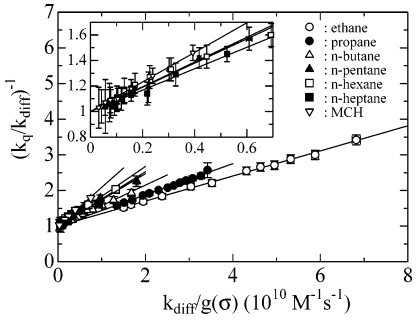

Figure 6. Plots of $(k_q/k_{diff})^{-1}$ against $k_{diff}/g(\sigma)$ in *n*-alkanes (C_2-C_7) and methylcyclohexane (MCH) at 25 °C.

D_i revealed that f_i decreases significantly with decreasing the solute size.[41,42]

Contribution of Diffusion to the Quenching. The plots of k_q/k_{diff} against k_{diff} in *n*-alkanes and MCH that give the degree of the contribution of diffusion to the quenching are shown in Figure 5. The values of k_q/k_{diff} at the lowest pressure measured in this and previous works were 0.29 in ethane (5.10 MPa), 0.39 in propane (2.12 MPa), and 0.52 in *n*-butane (3.0 MPa) and 0.44, 0.49, 0.61, and 0.56 in *n*-pentane, *n*-hexane, *n*-heptane, and MCH at 0.1 MPa; they increase monotonically with decreasing k_{diff} and approach unity in all of the solvents examined in this and previous works. The dependence of k_q/k_{diff} on k_{diff} may be explained by eq 16, which is derived from eqs 3 and 6.

$$\left(\frac{k_q}{k_{diff}}\right)^{-1} = \left(\frac{1}{k_{bim,0}}\right)\left(\frac{k_{diff}}{g(\sigma)}\right) + 1 \tag{16}$$

As seen in Figure 6, the plots of $(k_q/k_{diff})^{-1}$ against $k_{diff}/g(\sigma)$ are approximately linear with the intercept of unity. We also

evaluated $k_{bim,0}$ from the slopes in Figure 6 since the determination from the intercepts (Figure 3) may lead to large errors. The values of $k_{bim,0}$ determined are $(2.85 \pm 0.05) \times 10^{10}$, $(2.28 \pm 0.06) \times 10^{10}$, $(1.76 \pm 0.07) \times 10^{10}$, $(1.31 \pm 0.08) \times 10^{10}$, $(1.19 \pm 0.06) \times 10^{10}$, $(1.36 \pm 0.10) \times 10^{10}$, and $(0.92 \pm 0.03) \times 10^{10}$ M^{-1} s^{-1} in ethane, propane, *n*-butane, *n*-pentane, *n*-hexane, *n*-heptane, and MCH, respectively. They are in good agreement with the data shown in Table 2. Thus, the fluorescence quenching of DMEA by oxygen in *n*-alkanes and MCH is not fully but partially diffusion controlled, and the contribution of diffusion to the quenching is controlled by the radial distribution at contact, $g(\sigma)$, as well as the solvent viscosity, η.

k_{diff}/k_{-diff}. The value of $k_{bim,0}$ is the apparent bimolecular quenching rate constant in solvent cage, which was determined by extrapolating to $g(\sigma)\eta = 0$ in the plot of $g(\sigma)/k_q$ against $g(\sigma)\eta$, i.e., $k_{bim,0}$ is defined by $k^S(k_{diff}/k_{-diff})_{g(\sigma)\eta \to 0}$ as mentioned in Introduction section.

In general, according to the random walk theory, eq 17 holds

$$\langle r^2 \rangle_0 = 6D^0_{M^*O} t^0_{M^*O} \tag{17}$$

where $\langle r^2 \rangle_0$ and $D^0_{M^*O}$ are the mean square distance between the solute molecules and the relative diffusion coefficient at $g(\sigma)\eta \to 0$, respectively, and $t^0_{M^*O}$ $(= 1/k^0_{-diff})$ is the time that the two solute molecules $^1M^*$ and O_2 in the solvent cage reside within a distance of $\langle r^2 \rangle_0$. Therefore, the mean diameter of the solvent cage may be inferred to be $\langle r^2 \rangle_0^{1/2} + \sigma$.[43] At $g(\sigma)\eta \to 0$, we also obtain the following relationship for k^0_{diff} (see eq 12):

$$k^0_{diff} = 4\pi\sigma N_A D^0_{M^*O}/10^3 \tag{18}$$

From eqs 17 and 18, we have

$$(k_{diff}/k_{-diff})_0 = (2/3)\pi\sigma N_A \langle r^2 \rangle_0/10^3 \tag{19}$$

where $(k_{diff}/k_{-diff})_0$ represents k^0_{diff}/k^0_{-diff}.

As noted in Table 2, $k_{bim,0}$ decreases with increasing the radius of the solvent molecule, r_s, suggesting that $\langle r^2 \rangle_0$ depends on r_s if the unimolecular rate constant, k^S, is independent of solvent since $k_{bim,0} = k^S(k_{diff}/k_{-diff})_0$ (see eq 19). In this reasonable assumption that k^S is independent of solvent, $(k_{diff}/k_{-diff})_0$ in a given solvent may be expressed by

$$(k_{diff}/k_{-diff})_0 = (k_{diff}/k_{-diff})^{ref}_0 (k_{bim,0}/k^{ref}_{bim,0}) \tag{20}$$

In eq 20, the superscript "ref" represents the values in the solvent at $g(\sigma)\eta \to 0$ selected as a reference solvent. From eqs 19 and 20, we have

$$(k_{diff}/k_{-diff})_0 = (2/3)\pi\sigma N_A \langle r^2 \rangle^{ref}_0 (k_{bim,0}/k^{ref}_{bim,0})/10^3 \tag{21}$$

Unfortunately, there is no information about the relationship between $\langle r^2 \rangle_0$ and σ in liquid solvents. Therefore, we assume simply that $(\langle r \rangle^{2ref}_0)^{1/2} = \sigma$ for ethane that is the solvent with the lowest r_s examined in this work. In this case, the value of $(2/3)\pi\sigma\langle r \rangle^{2ref}_0/10^3$ $(=(k)_{diff}/k_{-diff^{ref}_0})$ in eq 21 was evaluated to be 0.195 M^{-1}. The values of $(k_{diff}/k_{-diff})_0$ obtained for the other solvents calculated by eq 21 are listed in Table 2, and those of k^S are also included in Table 2.

Once $(k_{diff}/k_{-diff})_0$ is determined for each solvent, we can calculate k_{diff}/k_{-diff} by eq 22 for a given solvent at an arbitrary pressure (solvent density) under the reasonable assumption that

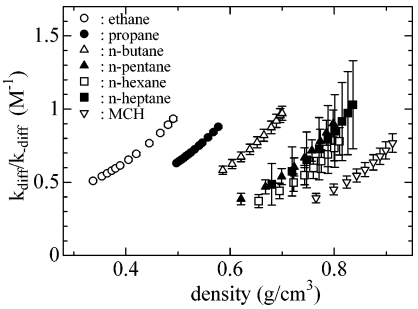

Figure 7. Plots of k_{diff}/k_{-diff} against solvent density in *n*-alkanes (C_2-C_7) and methylcyclohexane (MCH) at 25 °C.

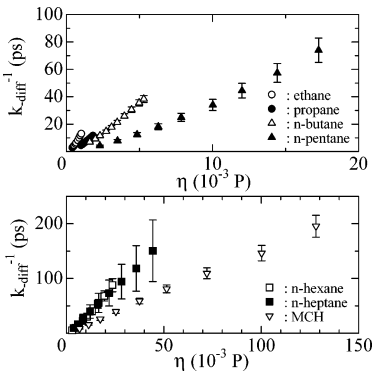

Figure 8. Plots of k_{-diff}^{-1} against solvent viscosity, η, in *n*-alkanes (C_2-C_7) and methylcyclohexane (MCH) at 25 °C.

k^S is independent of solvent and pressure.

$$k_{diff}/k_{-diff} = g(\sigma)(k_{diff}/k_{-diff})_0 \tag{22}$$

Figure 7 shows the density dependence of k_{diff}/k_{-diff} for the solvents examined in this work. It is noted in Figure 7 that k_{diff}/k_{-diff} increases significantly with increasing solvent density (pressure) in a given solvent. The values of k_{diff}/k_{-diff} at 0.1 MPa and 25 °C are 0.39 ± 0.04, 0.37 ± 0.05, 0.49 ± 0.15, and 0.39 ± 0.04 M^{-1} for *n*-pentane, *n*-hexane, *n*-heptane, and MCH, respectively; they are approximately independent of solvent within the error.

The values of k_{diff}/k_{-diff}, together with those k_{diff} mentioned above, lead to the evaluation of k_{-diff}. The solvent viscosity dependence of k_{-diff} is shown in Figure 8. The values of $1/k_{-diff}$ at 0.1 MPa and 25 °C are 4.2 ± 0.5, 5.2 ± 0.8, 9.3 ± 2.9, and 8.2 ± 0.7 ps in *n*-pentane, *n*-hexane, *n*-heptane, and MCH, respectively, and increase significantly with increasing solvent viscosity in all of the solvents examined in this work. This result of $1/k_{-diff}$, together with that of $1/k^S$ (6.9 ps; see Table 2) which is assumed to be independent of solvent and pressure (density), reveals that the quenching in the solvent cage approaches a fully diffusion-controlled rate as the solvent viscosity increases, being consistent with the conclusion as mentioned above.

Finally, the estimation of k_{diff}/k_{-diff} is very important for the analysis of the reaction kinetics with a nearly diffusion-controlled rate. Equation 23, which is independent of solvent, has been applied for many systems.[2,44]

$$k_{diff}/k_{-diff} = (4/3)\pi\sigma^3 \tag{23}$$

The value evaluated for the DMEA/O_2 system form eq 23 is 0.39 M^{-1}, which is very close to that at 0.1 MPa and 25 °C obtained in this work. However, the solvent density (pressure) dependence of k_{diff}/k_{-diff} cannot be predicted by eq 23. Another expression, which depends on solvent, is given from the

thermodynamic considerations by

$$k_{diff}/k_{-diff} = 1/[S] \quad (24)$$

where [S] is the molar concentration of the solvent.[45] According to eq 24, k_{diff}/k_{-diff} decreases with increasing pressure, but the experimental evidence in the present and previous works by us shows that k_{diff}/k_{-diff} is solvent-dependent and increases with increasing pressure. Thus, the pressure effect (solvent density effect) of k_{diff}/k_{-diff} at a given temperature cannot be explained by eqs 23 and 24.

Summary

The fluorescence quenching by oxygen of 9,10-dimethylanthracene (DMEA) in liquid ethane and propane has been investigated. From the solvent and pressure dependence of the quenching rate constant, k_q, together with the results in *n*-alkanes (C_2-C_7) and methylcyclohexane (MCH) that were previously reported, it was revealed clearly that the quenching is not fully but partially diffusion-controlled in agreement with our previous conclusion[6,17,19−22,24] and was found that the contribution of diffusion was successfully analyzed by eq 16. Finally, k_{diff}/k_{-diff} in *n*-alkanes (C_2-C_7) and MCH was evaluated by assuming that k^S is independent of the solvents examined in this work (see eq 21), and it was found that k_{diff}/k_{-diff} increases with increasing solvent density (Figure 7). From the results of k_{diff}/k_{-diff}, together with those of the solvent viscosity dependence of k_{diff} (Figure 4), it was found that k_{-diff} increasing significantly with increasing solvent viscosity (Figure 8).

Acknowledgment. This work is partly supported by Grant-in-Aid 17550010 to M.O.

References and Notes

(1) Birks, J. B. *Photophysics of Aromatic Molecules*; Wiley-Interscience: New York, 1970; p 518.
(2) Saltiel, J.; Atwater, B. W. *Advances in Photochemistry*; Wiley-Interscience: New York, 1987; Vol. 14, p 1.
(3) Ware, W. R. *J. Phys. Chem.* **1962**, *66*, 455.
(4) Birks, J. B. *Organic Molecular Photophysics*; Wiley: New York, 1973; p 403.
(5) Rice, S. A. In *Comprehensive Chemical Kinetics. Diffusion-Limited Reactions*; Bamford, C. H., Tripper, C. F. H., Compton, R. G., Eds; Elsevier: Amsterdam, 1985; Vol. 25.
(6) Schweitzer, C.; Schmidt, R. *Chem. Rev.* **2003**, *103*, 1685−1757.
(7) Yasuda, H.; Scully, A. D.; Hirayama, S.; Okamoto, M.; Tanaka, F. *J. Phys. Chem.* **1990**, *112*, 6847.
(8) Scully, A. D.; Yasuda, H.; Okamoto, M.; Hirayama, S. *Chem. Phys.* **1991**, *157*, 271.
(9) Scully, A. D.; Takeda, T.; Okamoto, M.; Hirayama, S. *Chem. Phys. Lett.* **1994**, *228*, 32.
(10) Pandey, K. K.; Okamoto, M.; Hirayama, S. *Chem. Phys. Lett.* **1994**, *224*, 417.
(11) Hirayama, S.; Yasuda, H.; Scully, A. D.; Okamoto, M. *J. Phys. Chem.* **1994**, *98*, 4609.
(12) El-Daly, S. A.; Okamoto, M.; Hirayama, S. *J. Photochem. Photobiol. A, Chem.* **1995**, *91*, 105.
(13) Okamoto, M.; Tanaka, F.; Hirayama, S. *J. Phys. Chem. A* **1998**, *102*, 10703.
(14) Okamoto, M. *J. Phys. Chem. A* **2000**, *104*, 5029.
(15) Okamoto, M. *J. Phys. Chem. A* **2000**, *104*, 7518.
(16) Okamoto, M.; Wada, O. *J. Photochem. Photobiol. A, Chem.* **2001**, *138*, 87.
(17) Okamoto, M.; Wada, O.; Tanaka, F.; Hirayama, S. *J. Phys. Chem. A* **2001**, *105*, 566.
(18) Okamoto, M.; Teratsuji, T.; Tazuke, Y.; Hirayama, S. *J. Phys. Chem. A* **2001**, *105*, 4574.
(19) Okamoto, M.; Yamada, K.; Nagashima, H.; Tanaka, F. *Chem. Phys. Lett.* **2001**, *342*, 578.
(20) Okamoto, M. *Phys. Chem. Chem. Phys.* **2001**, *3*, 3696.
(21) Okamoto, M. *Int. J. Thermophys.* **2002**, *23*, 421.
(22) Okamoto, M.; Tanaka, F. *J. Phys. Chem. A* **2002**, *106*, 3982.
(23) Okamoto, M.; Nagashima, H.; Tanaka, F. *Phys. Chem. Chem. Phys.* **2002**, *4*, 5627.
(24) Okamoto, M.; Tamai, T.; Tanaka, F. *J. Phys. Chem. A* **2003**, *107*, 1284.
(25) Okamoto, M. *J. Photochem. Photobiol. A, Chem.* **2004**, *162*, 17.
(26) Okamoto, M.; Teranishi, H. *J. Phys. Chem.* **1984**, *88*, 5644.
(27) Younglove, B. A.; Ely, J. F. *J. Phys. Chem. Ref. Data* **1987**, *16*, 577.
(28) Bridgman, P. W. *Proc. Am. Acad. Arts Sci.* **1926**, *61*, 57.
(29) Brazier, D. W.; Freeman, G, R. *Can. J. Chem.* **1969**, *47*, 893.
(30) Jonas, J.; Hasha, D.; Huang, S. G. *J. Chem. Phys.* **1979**, *71*, 3996.
(31) Kiran, E.; Sen, Y. L. *Int. J. Thermophys.* **1992**, *13*, 411.
(32) Diller, D. E.; Van Poolen, L. J. *Int. J. Thermophys.* **1985**, *6*, 43.
(33) Babb, S. E., Jr.; Scott, G. J. *J. Chem. Phys.* **1964**, *40*, 3666.
(34) Oliveiria, C. M. B. P.; Wakeham, W. A. *Int. J. Thermophys.* **1992**, *13*, 773.
(35) Collings, A. F.; McLaughlin, E. *Trans. Faraday. Soc.* **1971**, *67*, 340.
(36) Dymond, J. H.; Young, K. J.; Isdale, J. D. *Int. J. Thermophys.* **1980**, *1*, 345.
(37) Assael, M. J.; Oliveria, C. P.; Papadaki, M.; Wakeham, W. A. *J. Thermophys.* **1992**, *13*, 593.
(38) The radial distribution function at the closest approach distance, σ ($= r_{M^*} + r_O$) with the hard sphere assumption, $g(\sigma)$ is given by[39] $g(\sigma) = (1/1 - y) + (3y/(1 - y)^2)(r_{red}/r_S) + (2y^2/(1 - y)^3)(r_{red}/r_S))^2$ (eq A-1) where $r_{red} = r_{M^*}r_O/r_{M^*O}$, and y is the packing fraction, given in terms of the molar volume of solvent, V_S, by $y = (4N_A\pi r_S^3/3V_S)$ (eq A-2). By using the values of r_S, r_{M^*}, and r_O listed in Table 2, together with the data of the solvent density,[27−37] $g(\sigma)$ was calculated by eq A-1.
(39) Yoshimura, Y.; Nakahara, M. *J. Chem. Phys.* **1984**, *81*, 4080.
(40) Bondi, A. *J. Phys. Chem.* **1964**, *68*, 441.
(41) Evance, D. F.; Tominaga, T.; Chan, C. *J. Solution Chem.* **1979**, *8*, 461.
(42) Evance, D. F.; Tominaga, T.; Davis, H. T. *J. Chem. Phys.* **1981**, *74*, 1298.
(43) In this work, the solvent and solute molecules are assumed to be hard sphere; that is, the intermolecular potential between the solute molecules changes from zero to infinity at contact σ. So, the solvent caging may occur as a result of the cooperative pushing effect to the solute molecules by the solvent molecules.
(44) Lewis, C.; Ware, W. R. *Mol. Photochem.* **1973**, *5*, 261.
(45) Ref 2, and cited therein.